Electronic Supplementary Material (ESI) for New Journal of Chemistry.
This journal is © The Royal Society of Chemistry and the Centre National de la Recherche Scientifique 2023

Supporting information

Highly Stable Ni_8-Pyrazolate Metal-Organic Frameworks for Adsorption of Methylene Blue from Water

Guo-Qiang Wu, Kun Wu, Ying Wang, Jie Luo, Cong-Ying Zhou*, Weigang Lu*

College of Chemistry and Materials Science, and Guangdong Provincial Key Laboratory of Functional Supramolecular Coordination Materials and Applications, Jinan University, Guangzhou 510632, P. R. China

Corresponding Authors

E-mail: zhoucy2018@@jnu.edu.cn (Cong-Ying Zhou); weiganglu@jnu.edu.cn (Weigang Lu)

Content

Section 1. Materials and analytical techniques

All reagents and solvents were obtained commercially and used as received without further purification. Chemicals were purchased from Energy Chemical, Adamas-beta, Bidepharm, Merck, Sigma-Aldrich Co., Inc.

Powder X-ray diffraction (PXRD) data were collected on Rigaku Ultima IV diffractometer (40 kV, 40 mA, Cu Kα, λ = 1.5418 Å) from 5° to 30° with a step of 0.02° at a scan speed of 10° min^{-1}, and it was reduced to 2° min^{-1} for variable temperature powder X-ray diffraction (VT-PXRD) measurements. Thermogravimetric analysis (TGA) curves were obtained on Mettler-Toledo (TGA/DSC) thermal analyzer from 40 °C to 800 °C with a heating rate of 10 °C min^{-1} under a nitrogen gas atmosphere (20 $mL \cdot min^{-1}$). Fourier transform infrared (FT-IR) spectra were obtained on Thermo Scientific FT-IR Nicolet iS10 spectrophotometer in the range of 4000−400 cm^{-1}. UV−Visible (UV-Vis) absorption spectra were recorded on Agilent Cary 4000. N_2 adsorption/desorption measurements were performed on BELSORP-max II adsorption instrument. ^{1}H NMR (400 MHz) or (300 MHz) ^{13}C NMR (100 MHz) or (75 MHz) spectra spectra were recorded on a Bruker AVANCE III HD 400 spectrometer or Bruker 300 spectrometer using $CDCl_3$, DMSO as deuterated solvent.

Section 2. Synthesis of pyrazolate-based metallosalen

2.1 Synthesis of pyrazolate-based metallosalen (NiL_1, CuL_1)

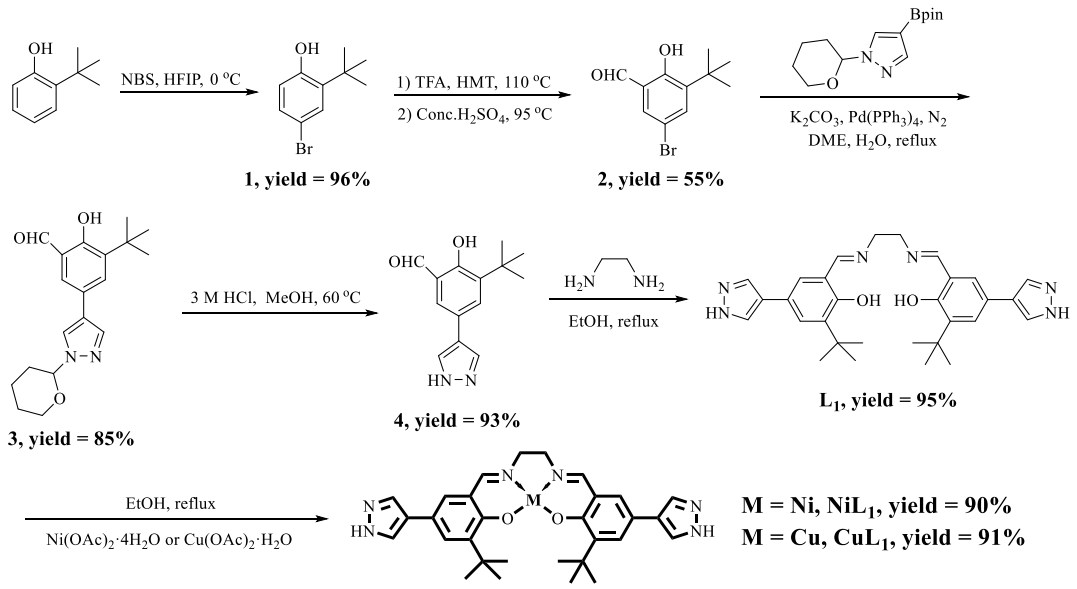

Scheme S1. The synthesis diagram of NiL_1 and CuL_1.

4-Bromo-2-tert-butylphenol (1). In a 250 mL single-necked flask, 2-tert-butylphenol (25.0 mmol, 3755.5 mg) and 35 mL of hexafluoroisopropanol (HFIP) were added, and then N-bromosuccinimide (NBS, 25.0 mmol, 4450.0 mg) was added after stirring for 20 min in an ice bath. The reaction was stired in an ice bath for 5 hours under air. Upon completion of the reaction, the solvent was evaporated under reduced pressure. Then the crude product obtained was purified by column chromatography on silica gel using 5% EA in PE to give a yellow oil (24.0 mmol, 5498.8 mg) in 96% yield. ^{1}H NMR (300 MHz, Chloroform-*d*) δ 7.35 (d, *J* = 2.4 Hz, 1H), 7.16 (dd, *J* = 8.4, 2.5 Hz, 1H), 6.56 (d, *J* = 8.4 Hz, 1H), 5.05 (s, 1H), 1.39 (s, 9H); ^{13}C NMR (75 MHz, Chloroform-*d*) δ 153.37, 138.70, 130.24, 129.67, 118.29, 113.02, 34.82, 29.44.

5-Bromo-3-tert-butyl-2-hydroxybenzaldehyde (2). Hexamethylenetetramine (HMT, 42.4 mmol, 5.9 g) was charged into a 250 mL round-bottom flask and dissolved by Triflouroacetic acid (30 mL). Compound **1** (21.2 mmol, 4.8 g) was then added and the solution was heated to reflux overnight. Then, 12 mL of 33% H_2SO_4 (w/w) was added to the reaction and the mixture was refluxed for 4 more hours. After completion of the

reaction, the solution was diluted with H_2O and extracted with a mixture of EA and PE (1:1, v/v). The organic layer was collected, dried over anhydrous $NaSO_4$ and concentrated on a rotavapor. The crude product was purified by column chromatography on silica gel (eluent: PE) to give a pale yellow solid (11.7 mmol, 2998.1 mg) with a yield of 55%. ^{1}H NMR (300 MHz, Chloroform-d) δ 11.72 (s, 1H), 9.81 (s, 1H), 7.58 (d, J = 2.5 Hz, 1H), 7.51 (d, J = 2.5 Hz, 1H), 1.40 (s, 9H); ^{13}C NMR (75 MHz, Chloroform-d) δ 196.16, 160.34, 141.26, 137.13, 133.74, 121.81, 111.27, 35.27, 29.13.

3-(tert-butyl)-2-hydroxy-5-(1-(tetrahydro-2H-pyran-2-yl)-1H-pyrazol-4-yl)benzaldehyde (3). Compound **2** (34.0 mmol, 8.7 g), boronic acid pinacol ester (40.7 mmol, 11.3 g), K_2CO_3 (102 mmol, 14.1 g), $Pd(PPh_3)_4$ (0.68 mmol, 786.0 mg) were charged into a 500 mL round-bottom flask and dissolved by degassed solvent (240 mL, DME/H_2O, 7/1) under nitrogen atmosphere. The reaction was then heated to reflux for 18 h. After completion of the reaction, the solution was diluted with H_2O and extracted with DCM (3×100 mL). The organic layer was collected, dried over anhydrous NaSO4 and concentrated on a rotavapor. The crude product was purified by column chromatography on silica gel (eluent: 10%EA in PE) to yield yellow solid (28.9 mmol, 9.5 g, yield = 85%). ^{1}H NMR (400 MHz, Chloroform-*d*) δ 11.71 (s, 1H), 9.87 (s, 1H), 7.82 (d, *J* = 0.8 Hz, 1H), 7.77 (d, *J* = 0.9 Hz, 1H), 7.61 (d, *J* = 2.2 Hz, 1H), 7.46 (d, *J* = 2.3 Hz, 1H), 5.40 (dd, *J* = 9.1, 3.2 Hz, 1H), 4.15 – 4.00 (m, 1H), 3.72 (ddd, *J* = 13.8, 7.9, 2.9 Hz, 1H), 2.21 – 1.99 (m, 3H), 1.75 – 1.57 (m, 3H), 1.43 (s, 9H); ^{13}C NMR (101 MHz, Chloroform-*d*) δ 197.17, 159.97, 138.79, 136.83, 132.02, 128.53, 124.10, 123.98, 122.58, 120.71, 87.89, 67.92, 34.94, 30.66, 29.23, 25.00, 22.44.

3-(tert-butyl)-2-hydroxy-5-(1H-pyrazol-4-yl)benzaldehyde (4). Compound **3** (30.0 mmol, 9.5 g) was suspended in 80 mL of MeOH. After stirring to dissolve, 60 mL of 3 M HCl (aq) was added to the solution, and the resulting solution was stirred at 60 °C for 10 h. The MeOH was evaporated in a rotary evaporator and the obtained mixture was neutralized by NH_4OH to pH = 7. The mixture was extracted with DCM or EA (5×100 mL), and then organic layer was collected, dried over anhydrous $NaSO_4$ and concentrated on a rotavapor. The crude product was purified by column

chromatography on silica gel (2%MeOH in DCM) to yield yellow solid (27.9 mmol, 6.8 g, yield = 93%). ^{1}H NMR (400 MHz, Chloroform-*d*) δ 9.92 (s, 1H), 7.86 (s, 2H), 7.66 (d, *J* = 2.3 Hz, 1H), 7.51 (d, *J* = 2.2 Hz, 1H), 1.46 (s, 7H); ^{13}C NMR (101 MHz, Chloroform-*d*) δ 197.25, 160.17, 139.07, 132.24, 130.96, 128.74, 123.95, 121.98, 120.83, 35.07, 29.32.

6,6'-((1E,1'E)-(ethane-1,2-diylbis(azaneylylidene))bis(methaneylylidene))bis(2-(tert-butyl)-4-(1H-pyrazol-4-yl)phenol) (L_1). The compound **4** (4.0 mmol, 977.2 mg) was charged into a 250 mL double-necked flask, and 100 mL of anhydrous ethanol was added and refluxed at 90 °C for 40 min with stirring, followed by the addition of ethylenediamine (140 μL, 2.0 mmol) to the system with a microsyringes, and then refluxed at 90 °C for 6 h. After the reaction, the yellow mixture is filtered, washed with anhydrous ethanol and dried in air overnight to obtain a bright yellow solid (1.9 mmol, 956.6 mg, yield = 95%). ^{1}H NMR (400 MHz, DMSO-d_6) δ 14.17 (s, 2H), 12.85 (s, 2H), 8.60 (s, 2H), 7.92 (s, 4H), 7.48 (s, 2H), 7.44 (s, 2H), 3.95 (s, 4H), 1.39 (s, 18H); ^{13}C NMR (101 MHz, DMSO-d_6) δ 167.81, 158.49, 136.87, 126.78, 126.49, 122.73, 121.10, 118.44, 58.37, 34.50, 29.22; HRMS: m/z: 513.3206 $[M+H]^+$.

Metallosalen complex (NiL_1). The compound L_1 (1.0 mmol, 513.0 mg) was charged into a 250 mL round-bottom flask and 80 mL of anhydrous ethanol was added. The obtained mixture was refluxed at 90 °C for 40 min with stirring, followed by the addition of $Ni(OAc)_2{\cdot}4H_2O$ (1.0 mmol, 250.0 mg), and then refluxed at 90 °C for 4 h. After the reaction, the mixture is filtered, washed with anhydrous ethanol and dried in air overnight to obtain a dark yellow solid (0.9 mmol, 510.0 mg, yield = 90%). ^{1}H NMR (400 MHz, DMSO-d_6) δ 12.77 (s, 2H), 8.04 – 7.71 (m, 6H), 7.33 (s, 4H), 3.42 (s, 4H), 1.37 (s, 18H); ^{13}C NMR (101 MHz, DMSO-d_6) δ 162.87, 161.86, 139.67, 128.17, 126.92, 121.46, 120.56, 118.42, 58.12, 35.16, 29.48; HRMS: m/z: 569.2205 $[M+H]^+$ (Calcd m/z 569.2175 for $[M+H]^+$) .FT-IR (KBr, cm^{-1}): 3422 (br), 3146 (m), 2923 (m), 1623 (s), 1532 (m), 1490 (w), 1442 (m), 1421 (m), 1394 (m), 1336 (m), 1299 (s), 1235 (w), 1171 (m), 954 (m), 858 (m), 810 (m), 779 (m), 726 (m), 710 (w), 603 (w), 508 (w) cm^{-1}.

Metallosalen complex (CuL_1). The synthesis procedure is similar to that of **NiL_1**

($Cu(OAc)_2·H_2O$ instead of $Ni(OAc)_2·4H_2O$). After reaction, dark gray solid was obtained (0.91 mmol, 522.8 mg, yield = 91%). Calcd for $C_{30}H_{34}N_6CuO_2$: C, 62.75; H, 5.97; N, 14.64. Found: C, 61.11; H, 5.33; N, 14.11; HRMS: m/z: 574.2147 $[M+H]^+$ (Calcd m/z 574.2118 for $[M+H]^+$). FT-IR (KBr, cm^{-1}): 3422 (br), 3167 (m), 2918 (m), 1628 (s), 1527 (m), 1447 (m), 1421 (w), 1389 (m), 1304 (m), 1230 (w), 1161 (m), 1039 (w), 1002 (w), 954 (w), 858 (w), 805 (m), 789 (m), 731 (m), 704 (m), 593 (w), 497 (m) cm^{-1}.

2.2 Synthesis of pyrazolate-based metallosalen (CuL_2).

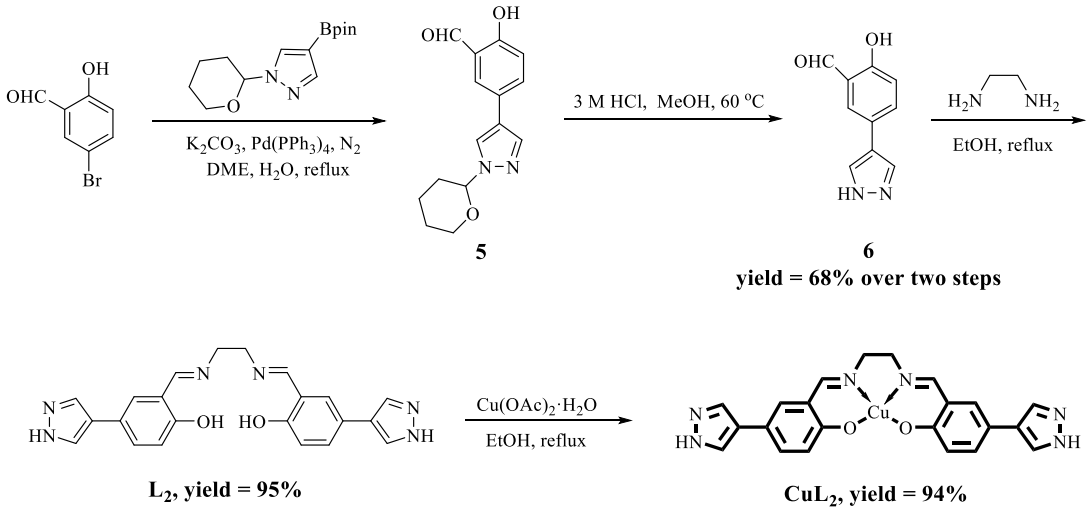

Scheme S2. The synthesis diagram of CuL_2.

2-Hydroxy-5-(1-(tetrahydro-2H-pyran-2-yl)-1H-pyrazol-4-yl)benzaldehyde (5). 5-Bromosalicylaldehyde (15.0 mmol, 3.0 g), boronic acid pinacol ester (18.0 mmol, 5.1 g), K_2CO_3 (45.0 mmol, 6.2 g), $Pd(PPh_3)_4$ (0.3 mmol, 346.7 mg) were charged into a 250 mL round-bottom flask and dissolved by degassed solvent (120 mL, DME/H2O, 7/1) under nitrogen atmosphere. The reaction was then heated to reflux for 18 h. After completion of the reaction, the solution was diluted with H_2O and extracted with DCM and EA (2×100 mL, respectively). The organic layer was collected, dried over anhydrous $NaSO_4$ and concentrated on a rotavapor. Since the solid obtained already has a high purity, the next reaction is carried out directly without further purification. ^1H NMR (400 MHz, Chloroform-*d*) δ 10.91 (s, 1H), 9.90 (s, 1H), 7.82 (s, 1H), 7.77 (s, 1H),

7.65 – 7.57 (m, 2H), 6.98 (d, J = 9.2 Hz, 1H), 5.40 (dd, J = 8.6, 3.8 Hz, 1H), 4.08 (dd, J = 12.6, 3.3 Hz, 1H), 3.79 – 3.65 (m, 1H), 2.16 – 1.99 (m, 3H), 1.72 – 1.60 (m, 3H); ^{13}C NMR (101 MHz, Chloroform-*d*) δ 196.64, 160.31, 136.82, 134.62, 130.28, 124.94, 124.23, 121.96, 120.77, 118.24, 87.92, 67.96, 30.67, 24.92, 22.45.

2-Hydroxy-5-(1H-pyrazol-4-yl)benzaldehyde (6). The above synthesized compound **5** was suspended in 60 mL of MeOH. After stirring to dissolve, 15 mL of 3 M HCl (aq) was added to the solution, and the resulting solution was stirred at 60 °C for 10 h. The MeOH was evaporated in a rotary evaporator and the obtained mixture was neutralized by NH_4OH to pH = 7. The mixture was extracted with DCM and EA (3×100 mL, respectively), and then organic layer was collected, dried over anhydrous $NaSO_4$ and concentrated on a rotavapor. The crude product was purified by column chromatography on silica gel using 100%EA to yield yellow solid (10.2 mmol, 1919.6 mg, two-step reaction yield = 68%). ^{1}H NMR (400 MHz, DMSO-d_6) δ 12.95 (br, 1H), 10.67 (s, 1H), 10.28 (s, 1H), 8.02 (s, 2H), 7.86 (d, J = 2.4 Hz, 1H), 7.76 (dd, J = 8.6, 2.4 Hz, 1H), 7.01 (d, J = 8.5 Hz, 1H); ^{13}C NMR (101 MHz, DMSO-d_6) δ 191.94, 159.15, 133.60, 125.34, 124.77, 122.46, 120.29, 117.86.

2,2'-((1E,1'E)-(ethane-1,2-diylbis(azaneylylidene))bis(methaneylylidene))bis(4-(1H-pyrazol-4-yl)phenol) (L_2). The compound **6** (2.0 mmol, 377.4 mg) was charged into a 250 mL double-necked flask, and 70 mL of anhydrous ethanol was added and refluxed at 90 °C for 15 min with stirring, followed by the addition of ethylenediamine (68 μL, 1.0 mmol) to the system with a microsyringes, and then refluxed at 90 °C for 6 h. After the reaction, the yellow mixture is filtered, washed with anhydrous ethanol and dried in air overnight to obtain a bright yellow solid (0.95 mmol, 380.1 mg, yield = 95%). ^{1}H NMR (400 MHz, DMSO-d_6) δ 13.25 (s, 2H), 12.82 (s, 2H), 8.60 (s, 2H), 7.94 (s, 4H), 7.67 (s, 2H), 7.56 (d, J = 8.5 Hz, 2H), 6.86 (d, J = 8.5 Hz, 2H), 3.95 (s, 2H); ^{13}C NMR (101 MHz, DMSO-d_6) δ 166.81, 158.82, 129.52, 127.99, 123.76, 120.54, 118.69, 116.86, 58.99; HRMS: m/z: 401.1750 $[M+H]^+$.

Metallosalen complex (CuL_2). The synthesis procedure is similar to that of **NiL_1** ($Cu(OAc)_2·H_2O$ instead of $Ni(OAc)_2·4H_2O$). After 12 h of reaction, green solid was obtained (0.94 mmol, 434.3 mg, yield = 94%). HRMS: m/z: 462.0851 $[M+H]^+$ (Calcd

m/z 462.0865 for $[M+H]^+$). FT-IR (KBr, cm^{-1}): 3427 (br), 3178 (m), 2955 (m), 1638 (s), 1591 (w), 1564 (w), 1490 (m), 1283 (m), 1192 (m), 1039 (m), 975 (m), 959 (m), 853 (m), 810 (m), 773 (w), 694 (w), 635 (w), 582 (w) cm^{-1}.

Section 3. Characterization of Ni_8-NiL_1, Ni_8-CuL_1, Ni_8-CuL_2

3.1 Structural analysis

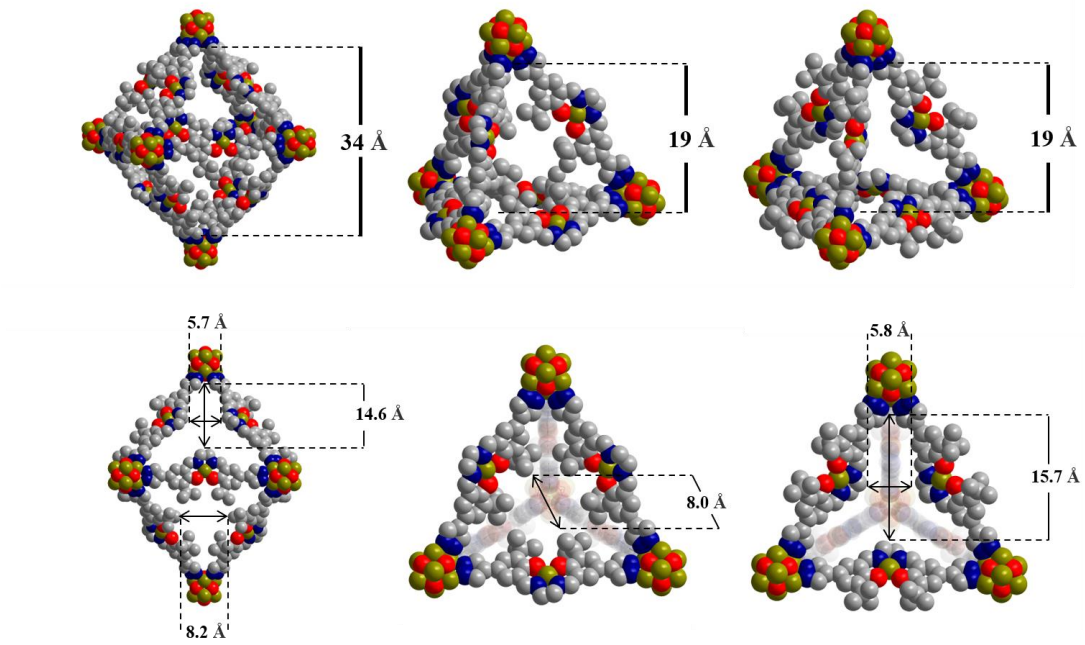

Fig. S1 Space-filling diagram of the tetrahedral and octahedral cages of Ni_8-NiL_1 (top). The diagram of the size of triangular-like windows of cages (bottom).

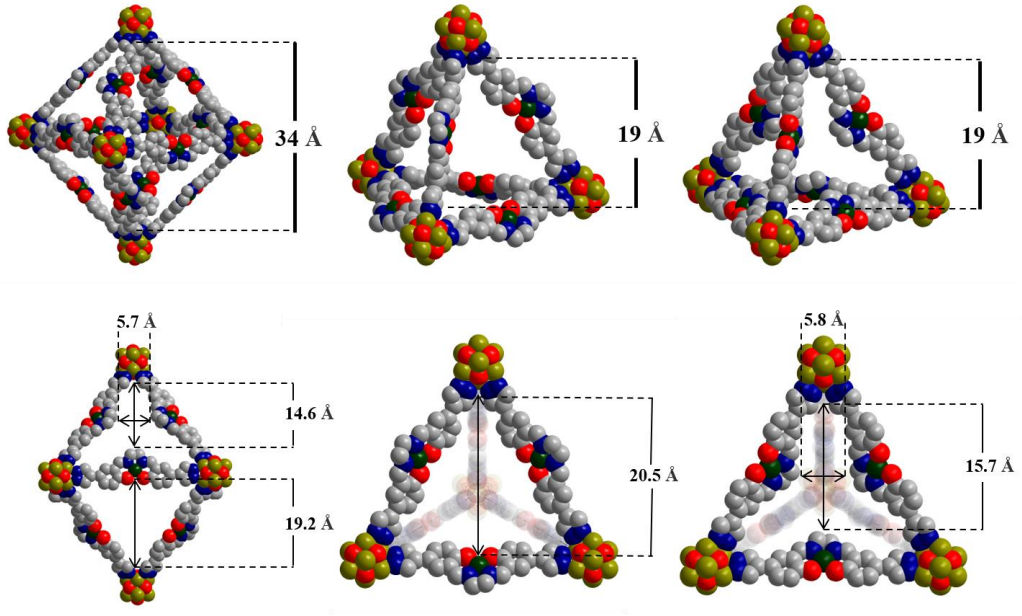

Fig. S2 Space-filling diagram of the tetrahedral and octahedral cages of Ni_8-CuL_2 (top). The diagram of the size of triangular-like windows of cages (bottom).

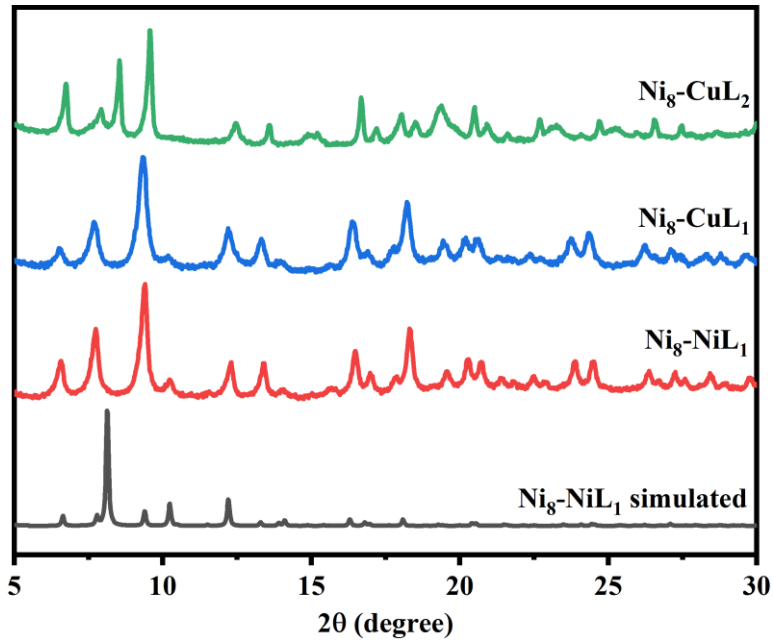

Fig. S3 The simulated PXRD patterns of Ni_8-NiL_1 and as-synthesized PXRD patterns of Ni_8-NiL_1, Ni_8-CuL_1 and Ni_8-CuL_2.

3.2 Stability and N_2 Adsorption

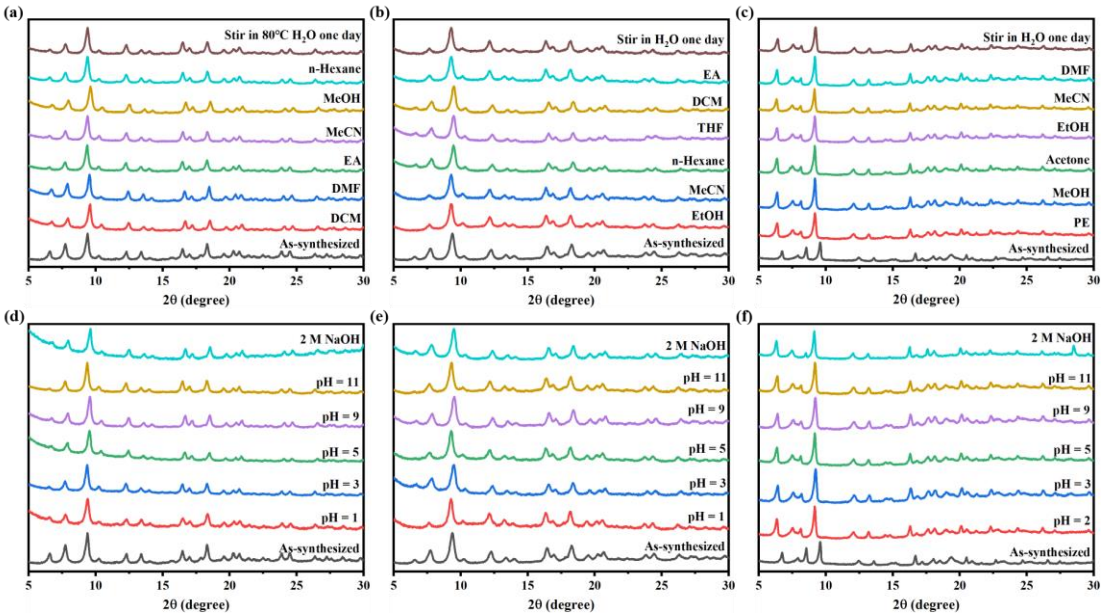

Fig. S4 The stability test of (a, d) Ni_8-NiL_1, (b, e) Ni_8-CuL_1, (c, f) Ni_8-CuL_2 under different conditions (be characterized by PXRD).

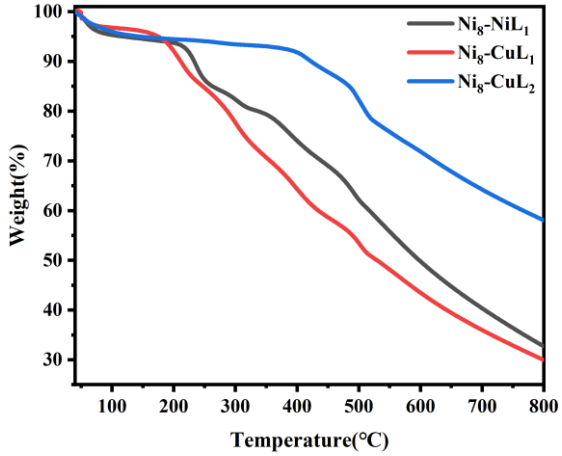

Fig. S5 Thermogravimetric analysis (TGA) of Ni_8-NiL_1, Ni_8-CuL_1 and Ni_8-CuL_2.

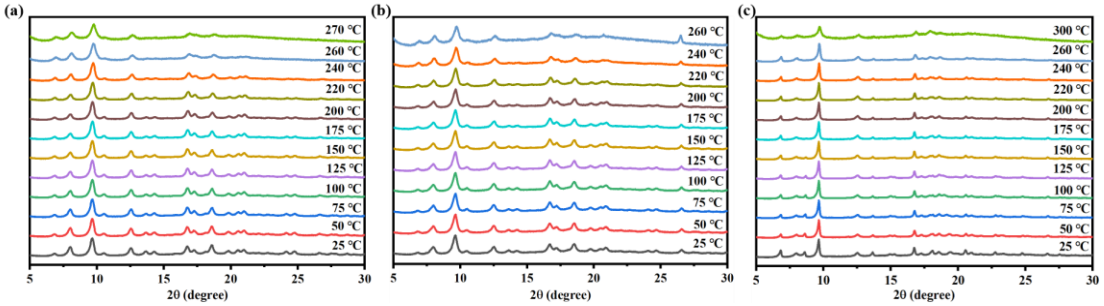

Fig. S6 The variable-temperature PXRD patterns of (a) Ni_8-NiL_1, (b) Ni_8-CuL_1, (c) Ni_8-CuL_2.

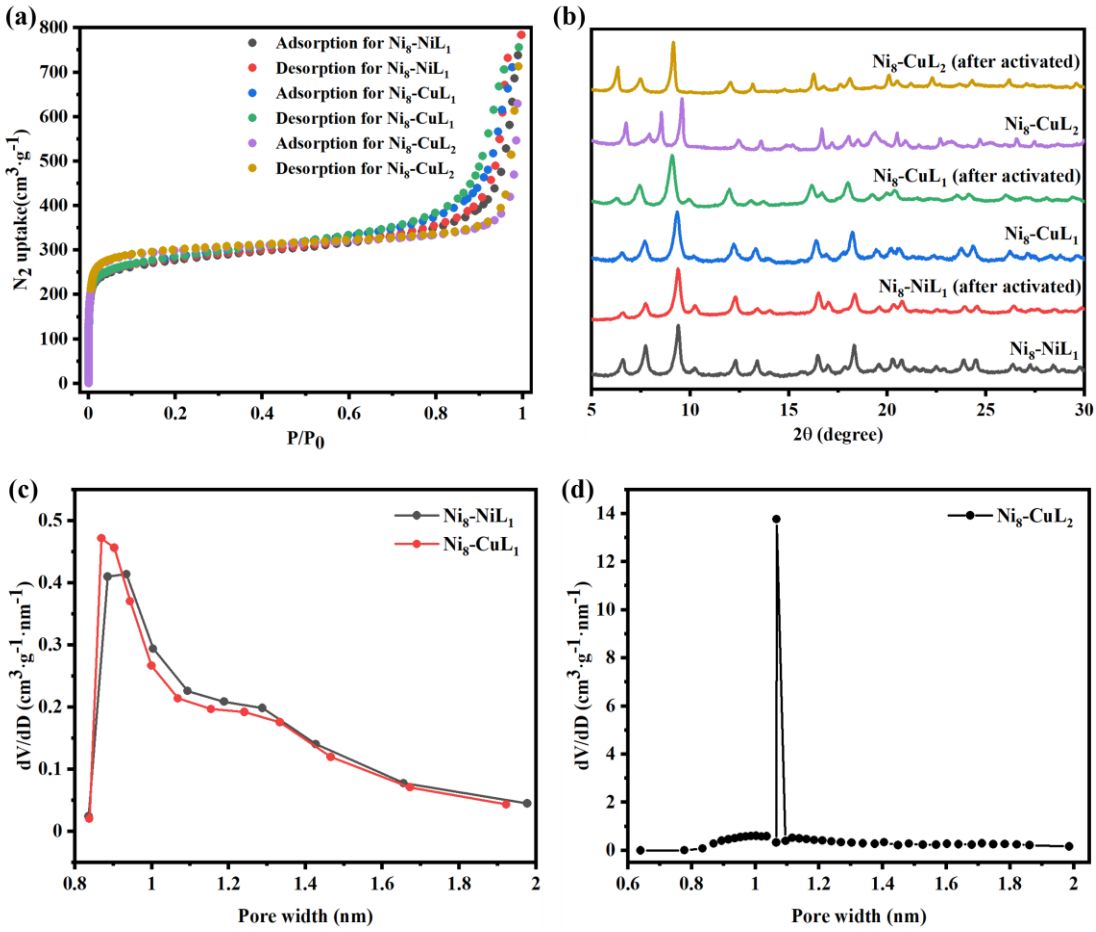

Fig. S7 (a) N_2 adsorption isotherms of Ni_8-NiL_1, Ni_8-CuL_1 and Ni_8-CuL_2 at 77 K. (b) The as-synthesized and activated PXRD patterns of Ni_8-NiL_1, Ni_8-CuL_1 and Ni_8-CuL_2. The pore size distributions of (c) Ni_8-NiL_1, Ni_8-CuL_1 and (d) Ni_8-CuL_2, calculated by the Saito-Foley method.

Section 4. Adsorption of organic dyes

4.1 Organic dyes in this work

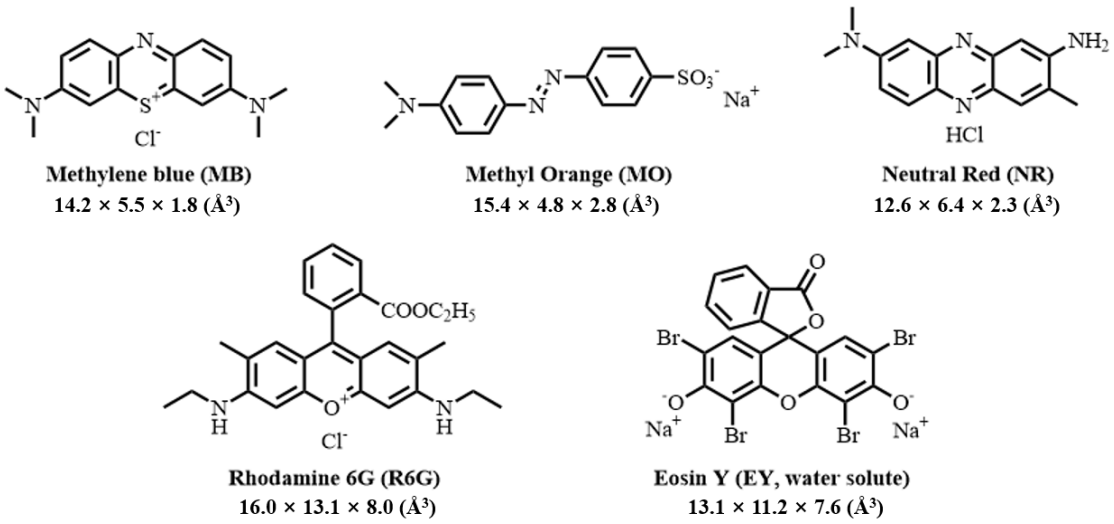

Fig. S8 Schematic structural illustration of dyes studied in this work. (The molecular sizes of the organic dyes were referred to the reported literature). [1, 2]

4.2 The standard curves of MB

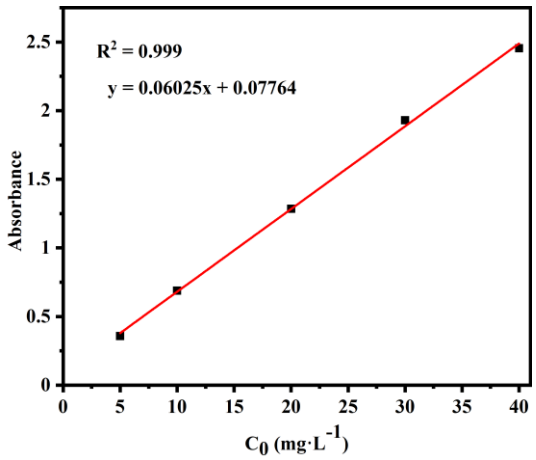

Fig. S9 The relationship between the absorbed intensity of MB and different concentrations by linear fitting.

4.3 UV-vis spectra of adsorption experiments

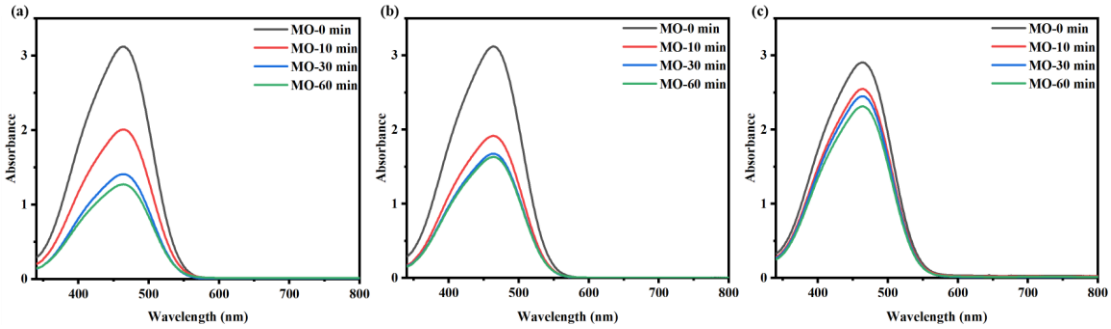

Fig. S10 UV-Vis spectra of aqueous solution of MO in the presence of (a) Ni_8-NiL_1, (b) Ni_8-CuL_1, (c) Ni_8-CuL_2 at different times.

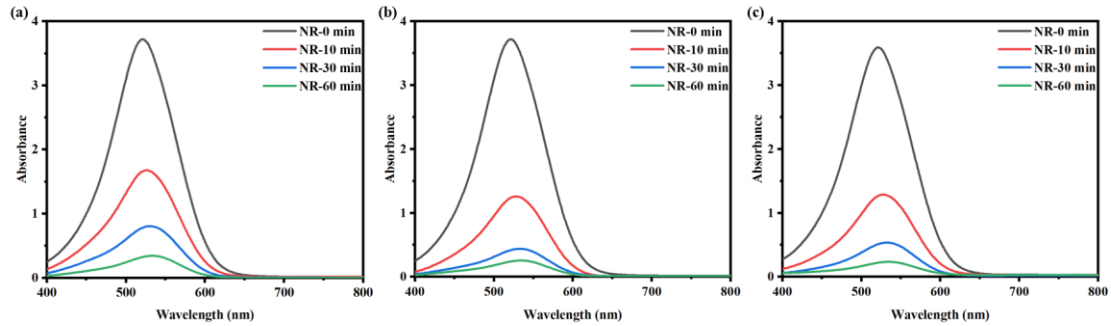

Fig. S11 UV-Vis spectra of aqueous solution of NR in the presence of (a) Ni_8-NiL_1, (b) Ni_8-CuL_1, (c) Ni_8-CuL_2 at different times.

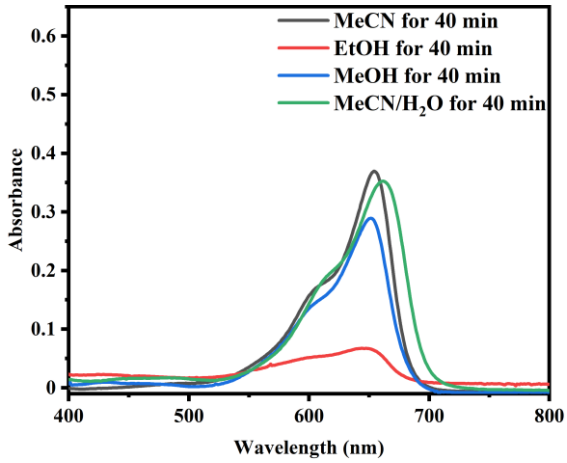

Fig. S12 UV-Vis spectral analysis of MB solution after dye-releasing experiments with MB@Ni_8-CuL_1 in different elution solvents.

4.4 The fitting parameters of adsorption kinetics

Table S1. The kinetic parameters for MB on Ni_8-NiL_1, Ni_8-CuL_1, Ni_8-CuL_2.

Sample	$Q_{e,exp}$ mg g^{-1}	Pseudo-first-order			Pseudo-second-order		
		$Q_{e,cal}$ mg g^{-1}	k_1 min^{-1}	R^2	$Q_{e,cal}$ mg g^{-1}	k_2 (g mg^{-1}) min^{-1}	R^2
Ni_8-NiL_1	396.8	388.1	0.032	0.97	**438.6**	**1.16×10^{-4}**	**0.99**
Ni_8-CuL_1	395.0	381.0	0.039	0.97	**427.4**	**1.51×10^{-4}**	**0.98**
Ni_8-CuL_2	**393.6**	**426.7**	**0.013**	**0.98**	480.8	4.0×10^{-5}	0.89

4.5 The fitting parameters of the adsorption isotherm

Table S2. The fitting results of the Langmuir model and Freundlich model for adsorption of MB on Ni_8-NiL_1, Ni_8-CuL_1, Ni_8-CuL_2.

Sample	Langmuir model			Freundlich model		
	$Q_{m,cal}$ mg g^{-1}	b L mg^{-1}	R^2	K_f (mg g^{-1})/(L mg^{-1})$^{1/n}$	$1/n$	R^2
Ni_8-N iL_1	**892.8**	**0.331**	**0.99**	720.83	0.036	0.95
Ni_8-CuL_1	**892.8**	**0.405**	**0.99**	725.62	0.036	0.97
Ni_8-CuL_2	**1034.0**	**0.121**	**0.99**	662.5	0.076	0.88

4.6 Summary of maximum adsorption amount of MB

Table S3. Comparison of maximum adsorption capacities (Q_e) of other materials for MB.

Adsorbent	Q_e (mg g^{-1})	Reference
Fe_3O_4@SiO_2 based organic polymers	1153	3
Sulfonated lignin-based hydrogels	540.5	4
Modified montmorillonite	781.3	5
Polyaminocarboxylated hydrochar from bamboo	1249.0	6
AC from cashew shell	476.0	7
AC from tomato waste	400.0	8
AC from watermelon rind	300.0	9
Graphene oxide/Fe_3O_4	1429.0	10
Bentonite/alginate	2024.0	11

4.7 Studies on adsorption mechanisms

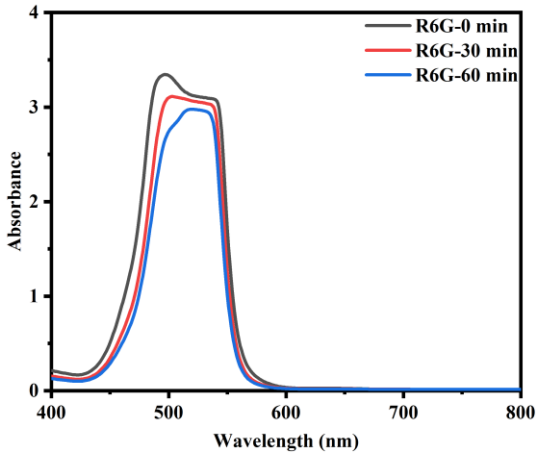

Fig. S13 UV-Vis spectra of aqueous solution of R6G in the presence of Ni_8-CuL_1 at different times.

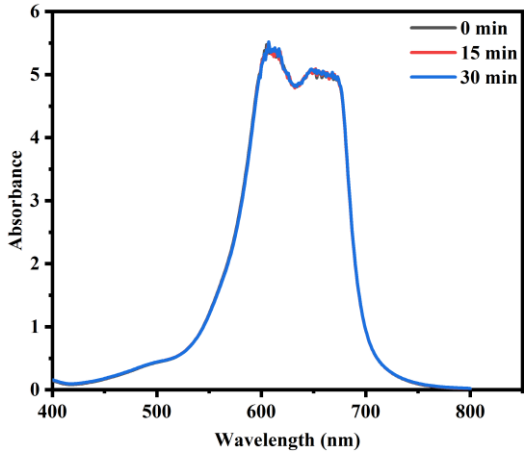

Fig. S14 UV-Vis spectra of aqueous solution of MB in the presence of ligand CuL_1 at different times.

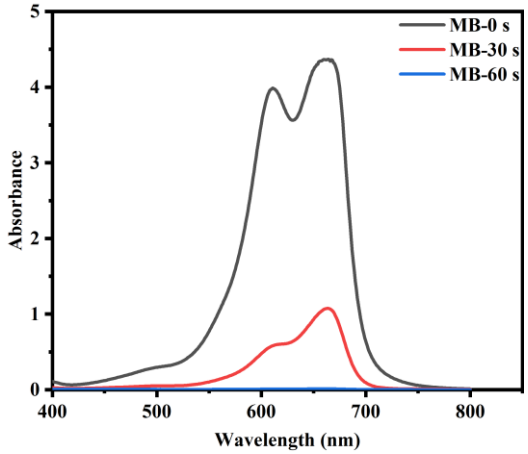

Fig. S15 UV-Vis spectra of aqueous solution of MB in the presence of Ni_8-CuL_1 under ultrasound.

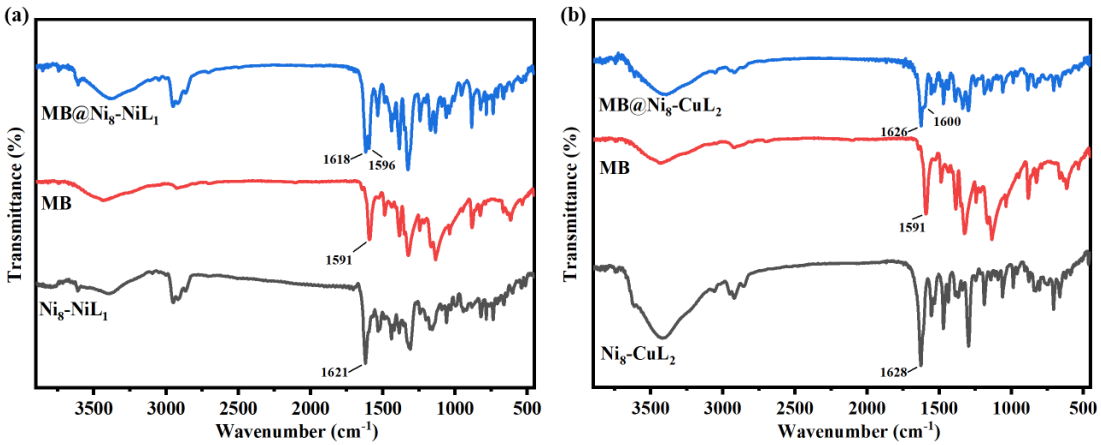

Fig. S16 (a) FT-IR spectra of MB, Ni_8-NiL_1 and MB@Ni_8-NiL_1. (b) FT-IR spectra of MB, Ni_8-CuL_2 and MB@Ni_8-CuL_2.

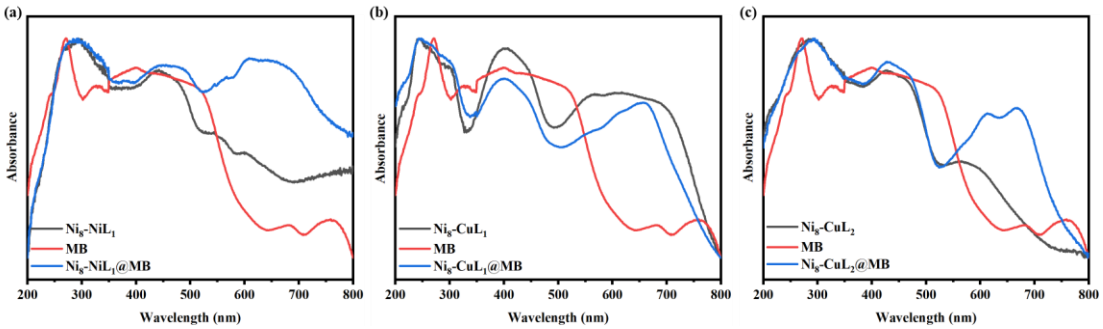

Fig. S17 (a, b, c) Solid-state UV-Vis spectra of MB molecule and Ni_8-CuL_1, Ni_8-CuL_1, Ni_8-CuL_2 before and after loaded with MB, respectively.

Appendix

^{1}H and ^{13}C NMR spectra for pyrazolate-based ligand and intermediate compound.

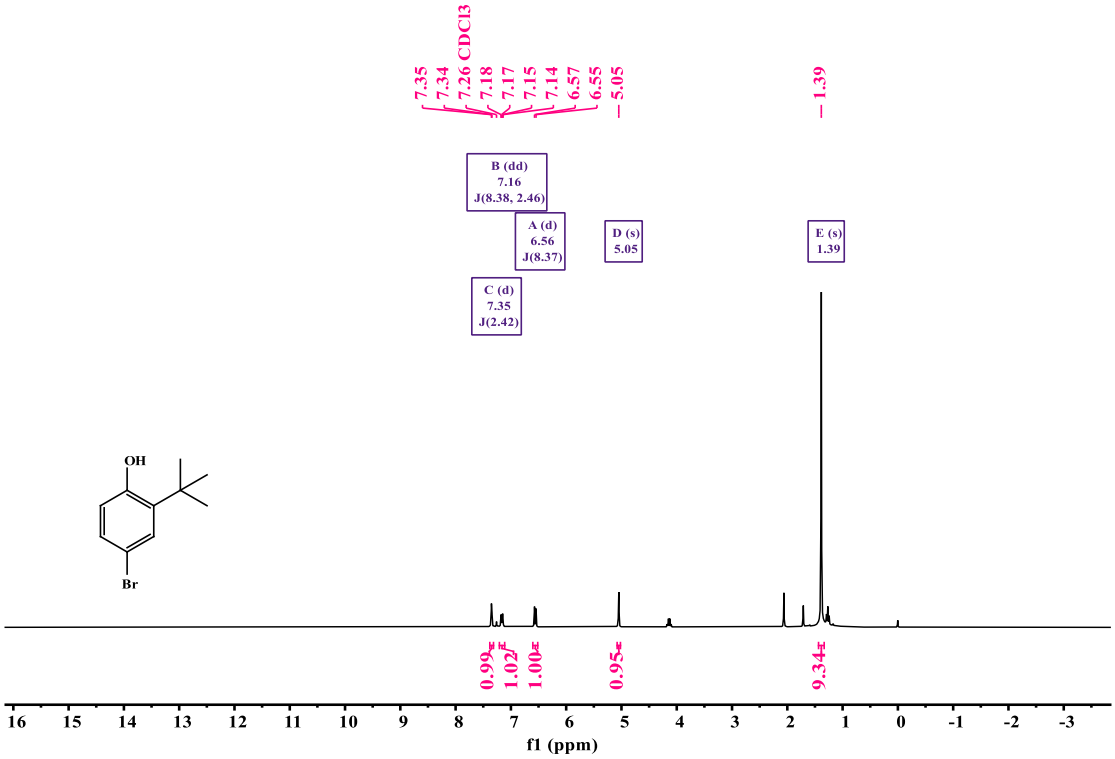

^{1}H spectra of 4-Bromo-2-tert-butylphenol (1).

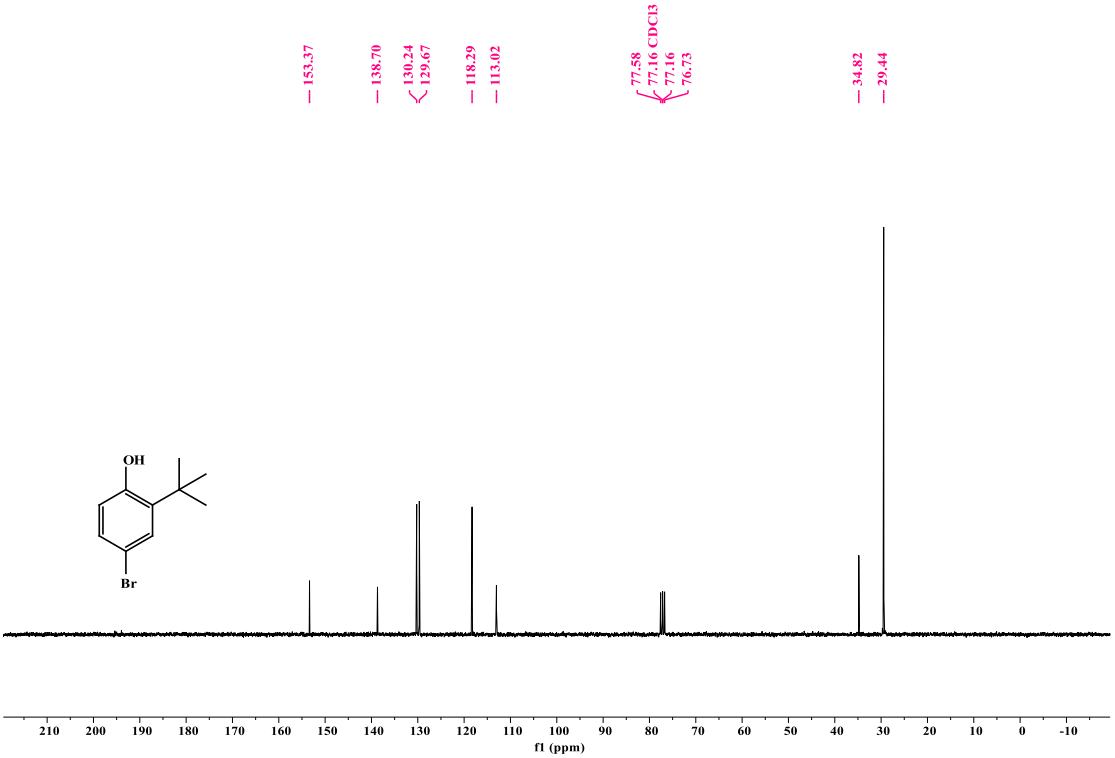

^{13}C spectra of 4-Bromo-2-tert-butylphenol (1).

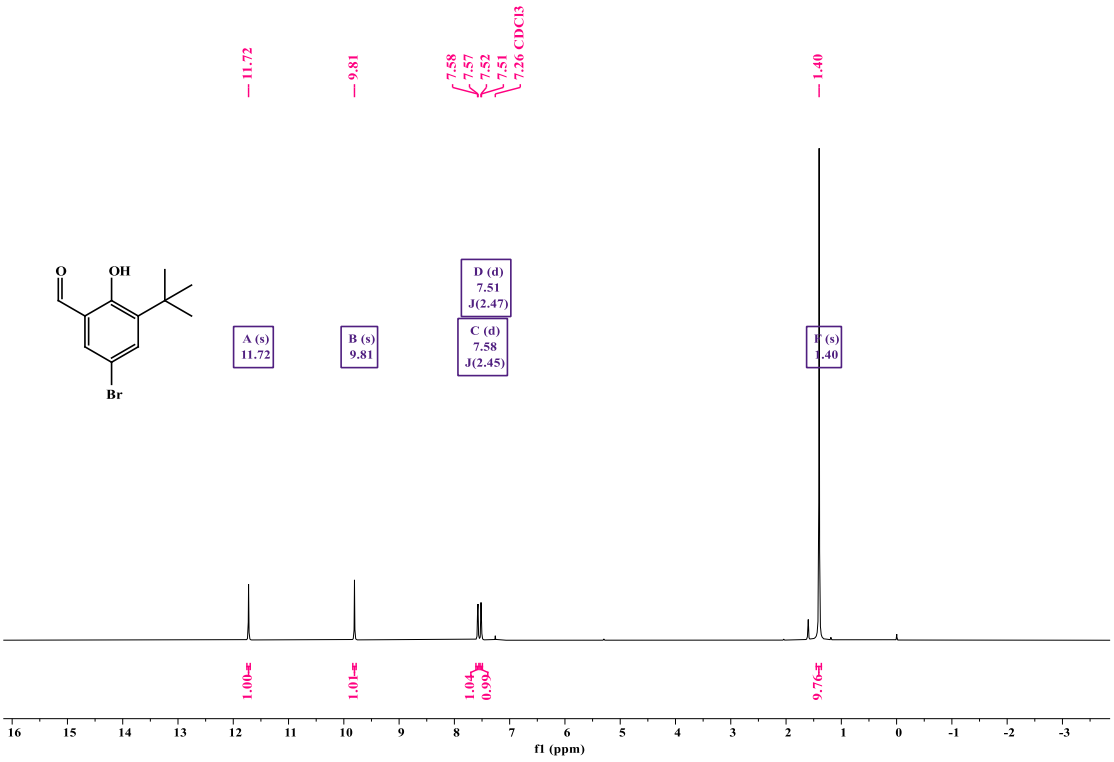

^{1}H spectra of 5-Bromo-3-tert-butyl-2-hydroxybenzaldehyde (2).

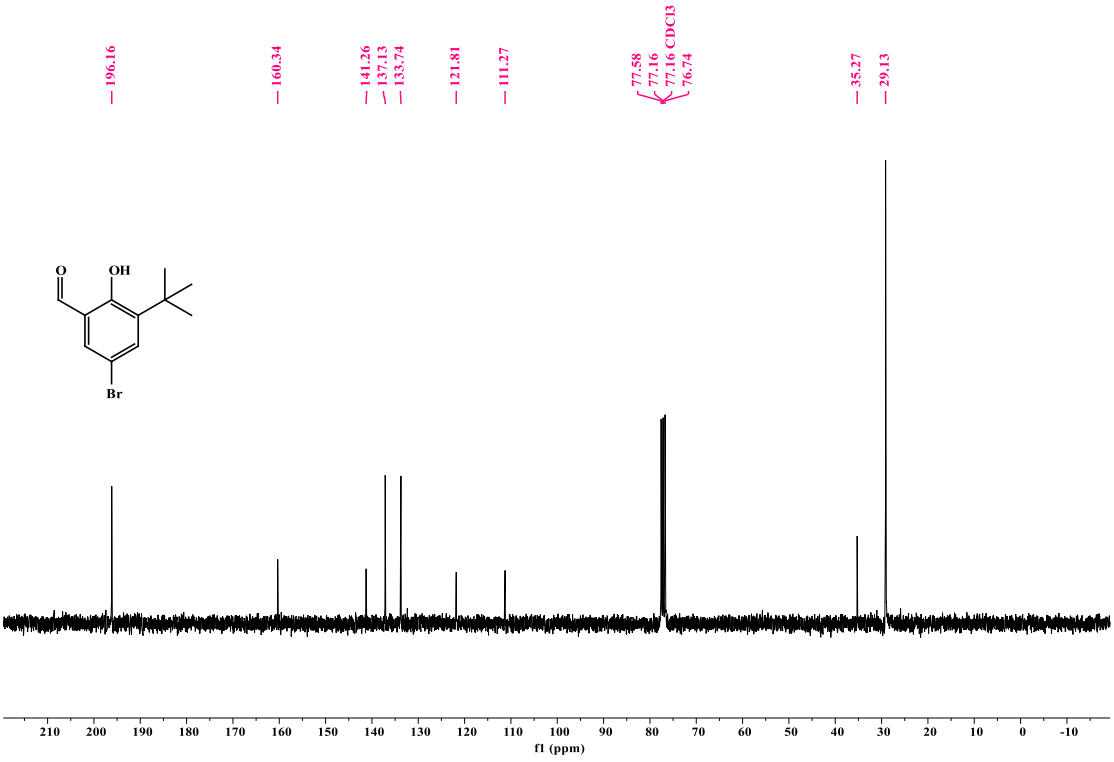

^{13}C spectra of 5-Bromo-3-tert-butyl-2-hydroxybenzaldehyde (2).

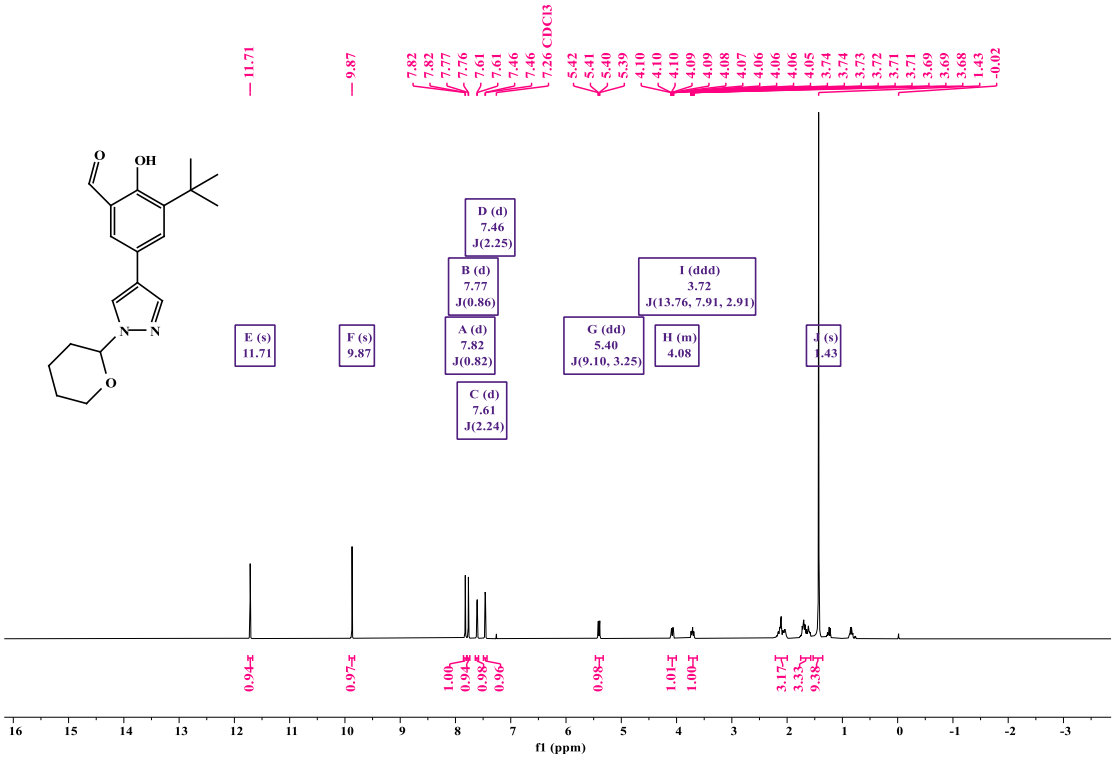

^{1}H spectra of 3-(tert-butyl)-2-hydroxy-5-(1-(tetrahydro-2H-pyran-2-yl)-1H-pyrazol-4-yl)benzaldehyde (3).

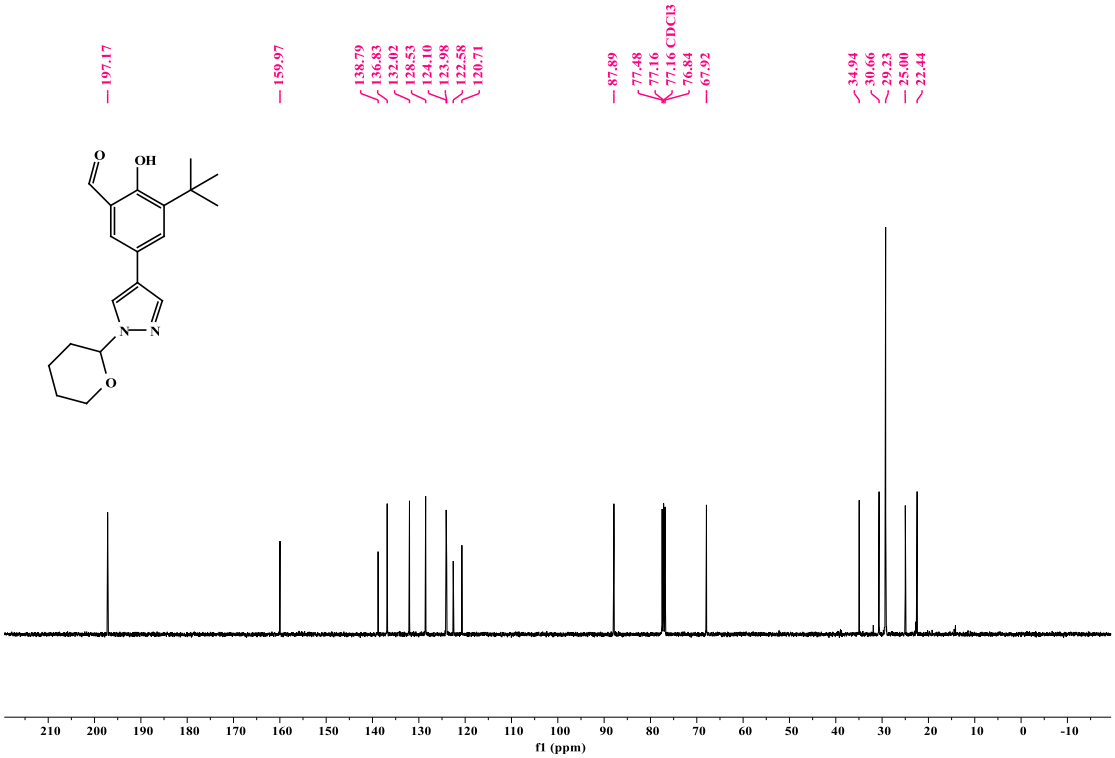

^{13}C spectra of 3-(tert-butyl)-2-hydroxy-5-(1-(tetrahydro-2H-pyran-2-yl)-1H-pyrazol-4-yl)benzaldehyde (3).

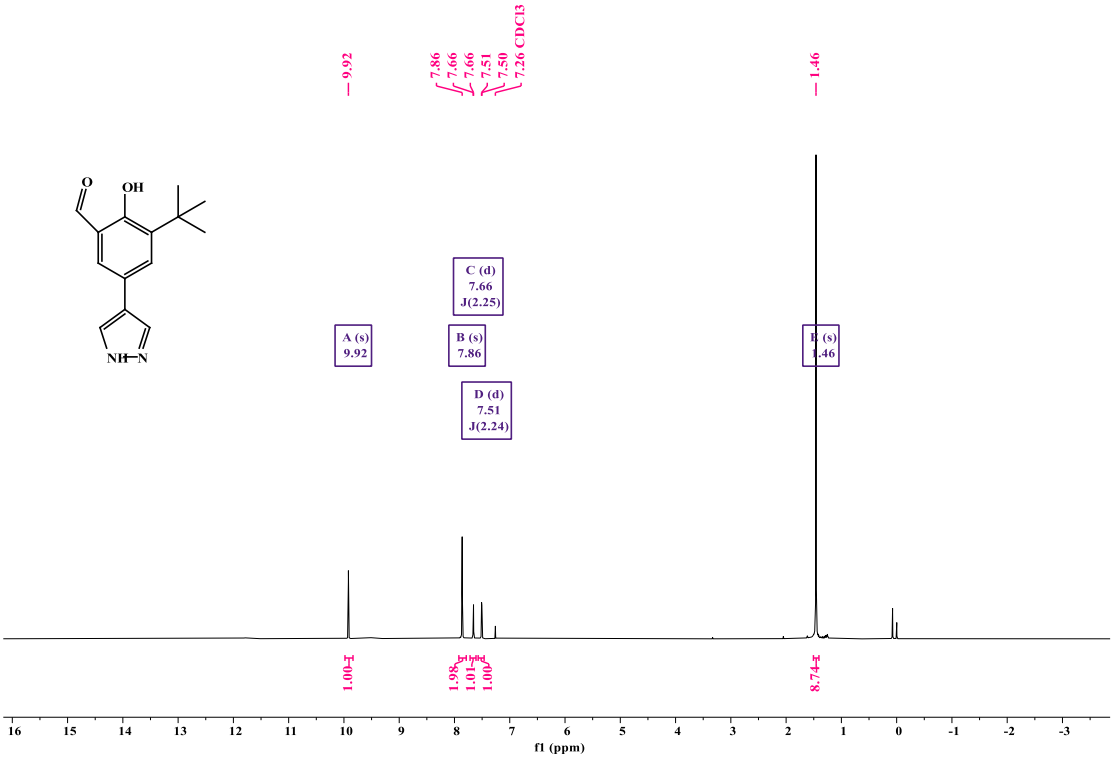

^{1}H spectra of 3-(tert-butyl)-2-hydroxy-5-(1H-pyrazol-4-yl)benzaldehyde (4).

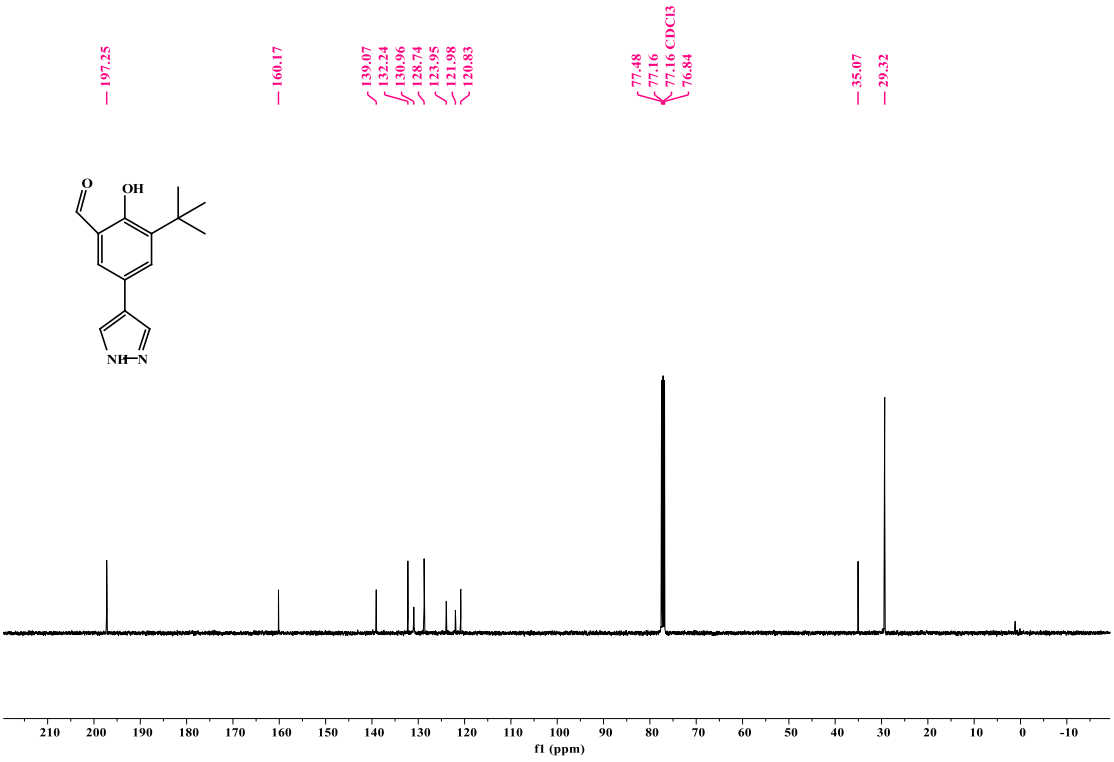

^{13}C spectra of 3-(tert-butyl)-2-hydroxy-5-(1H-pyrazol-4-yl)benzaldehyde (4).

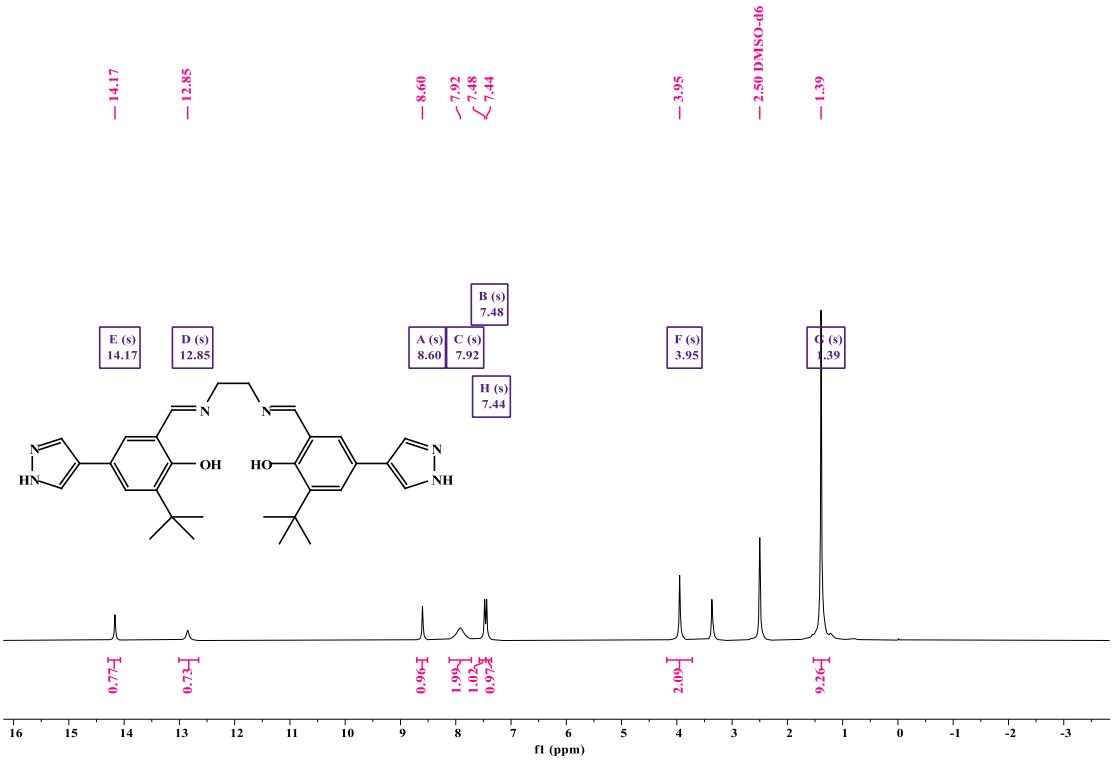

^{1}H spectra of 6,6'-((1E,1'E)-(ethane-1,2-diylbis(azaneylylidene))bis(methaneylylidene))bis(2-(tert-butyl)-4-(1H-pyrazol-4-yl)phenol) (L_1).

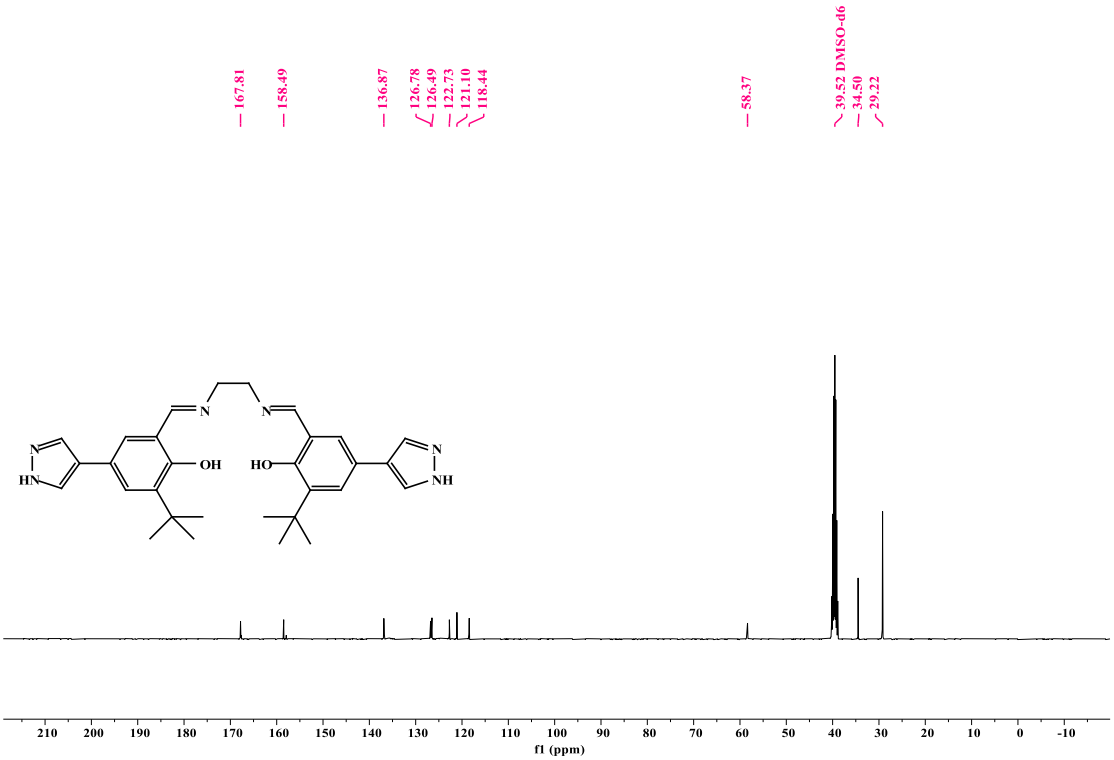

^{13}C spectra of 6,6'-((1E,1'E)-(ethane-1,2-diylbis(azaneylylidene))bis(methaneylylidene))bis(2-(tert-butyl)-4-(1H-pyrazol-4-yl)phenol) (L_1).

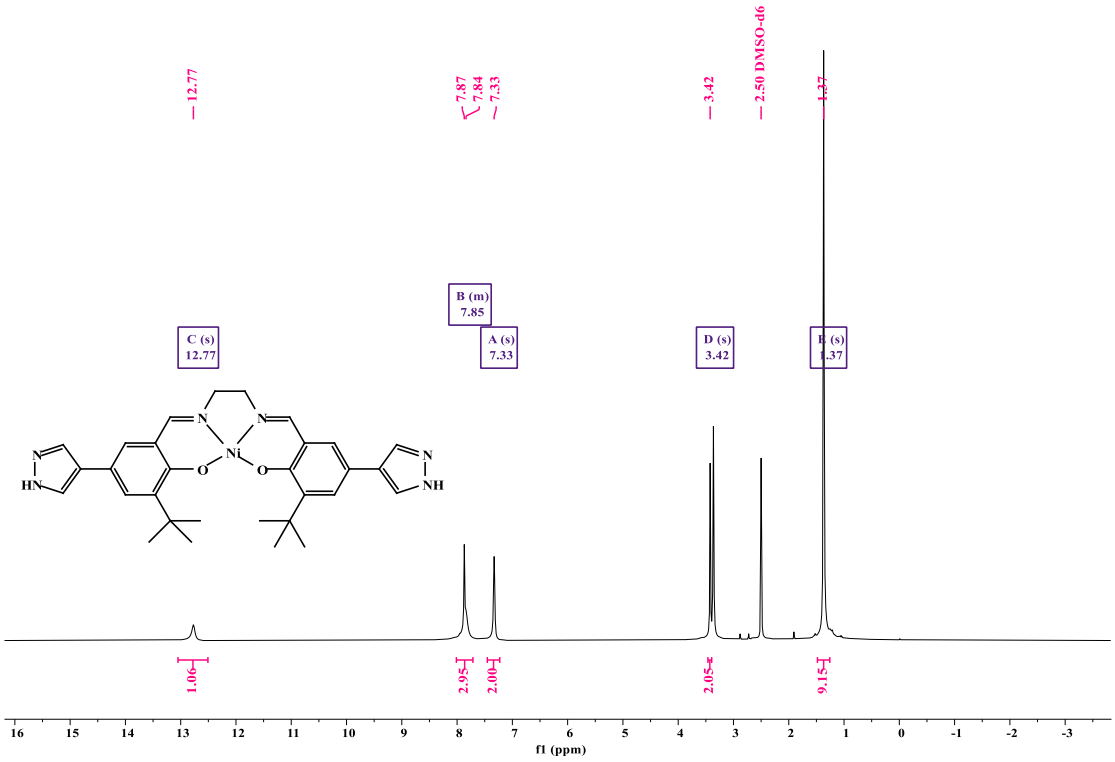

^{1}H spectra of Metallosalen complex (NiL$_1$).

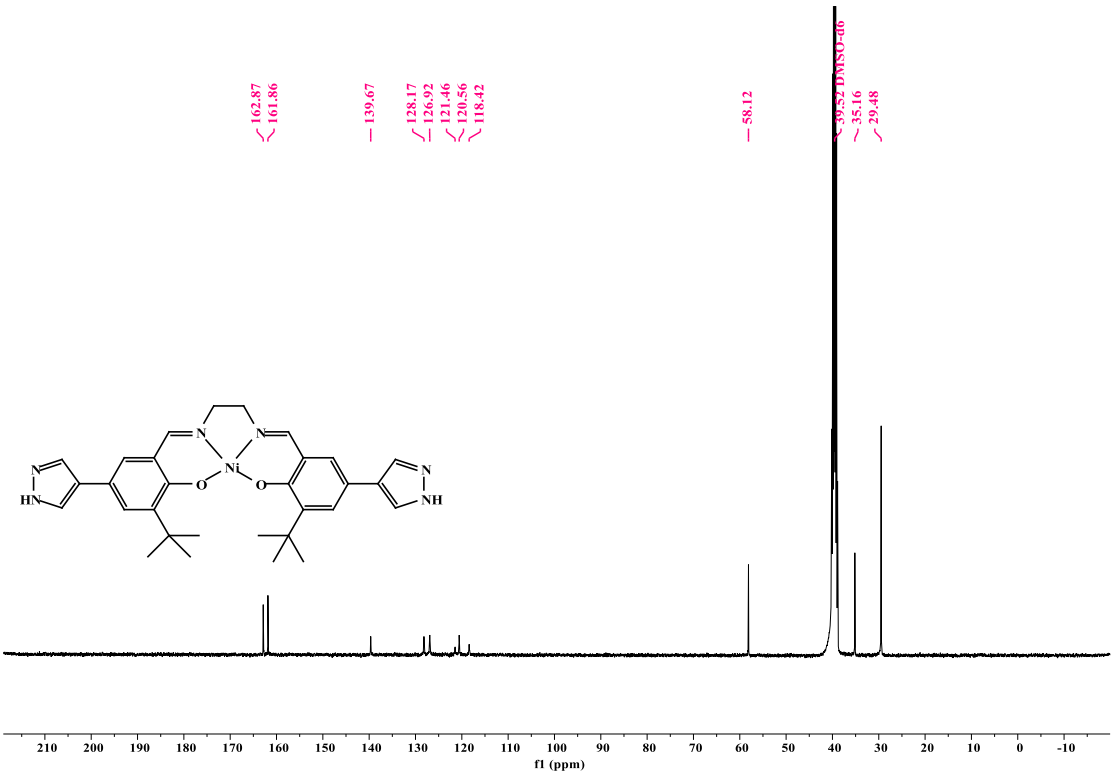

^{13}C spectra of Metallosalen complex (NiL$_1$).

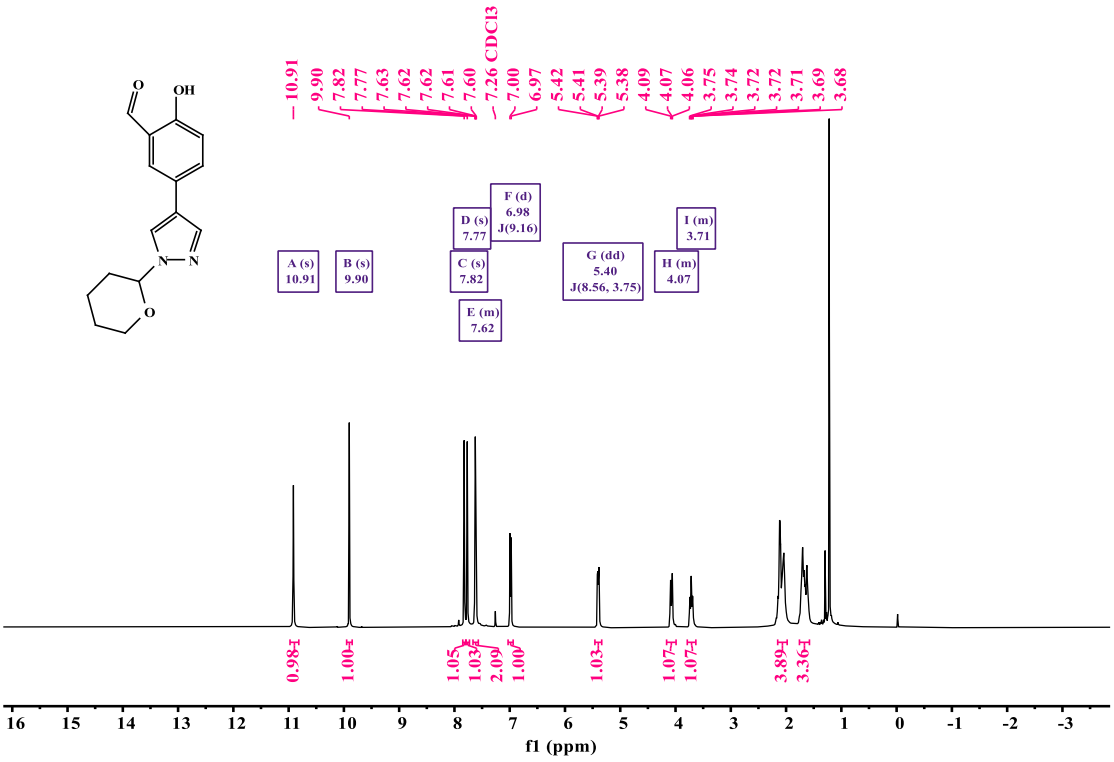

^{1}H spectra of 2-Hydroxy-5-(1-(tetrahydro-2H-pyran-2-yl)-1H-pyrazol-4-yl)benzaldehyde (5).

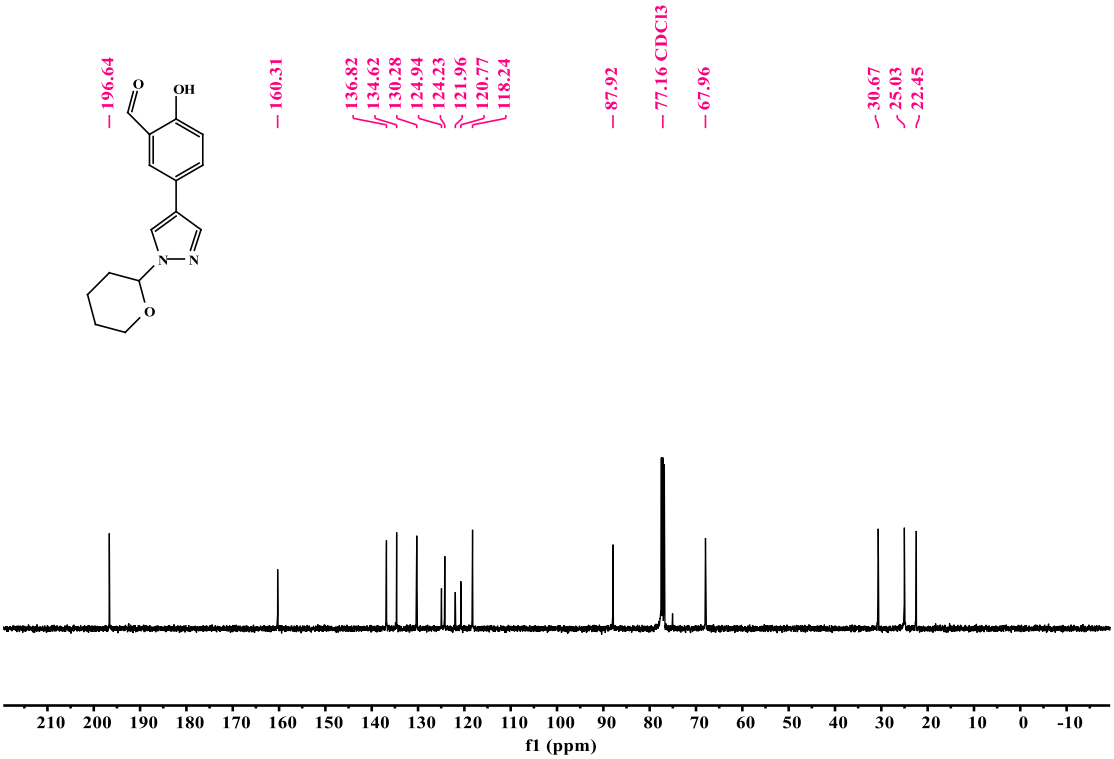

^{13}C spectra of 2-Hydroxy-5-(1-(tetrahydro-2H-pyran-2-yl)-1H-pyrazol-4-yl)benzaldehyde (5).

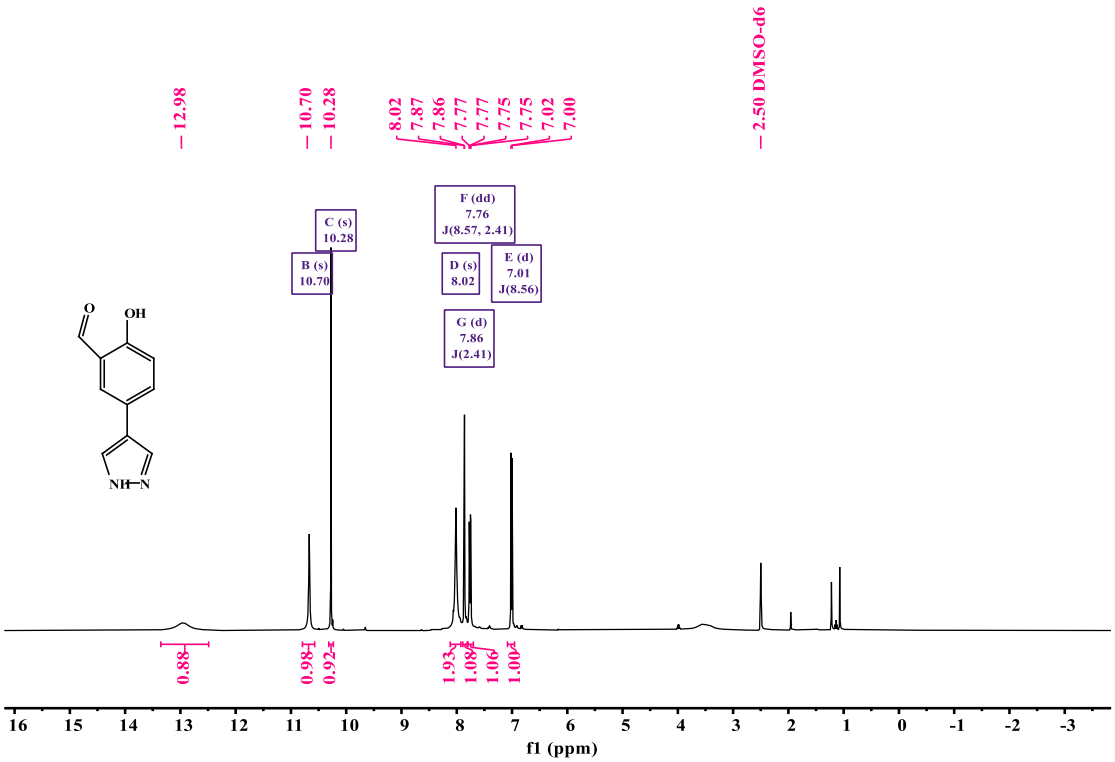

^{1}H spectra of 2-Hydroxy-5-(1H-pyrazol-4-yl)benzaldehyde (6).

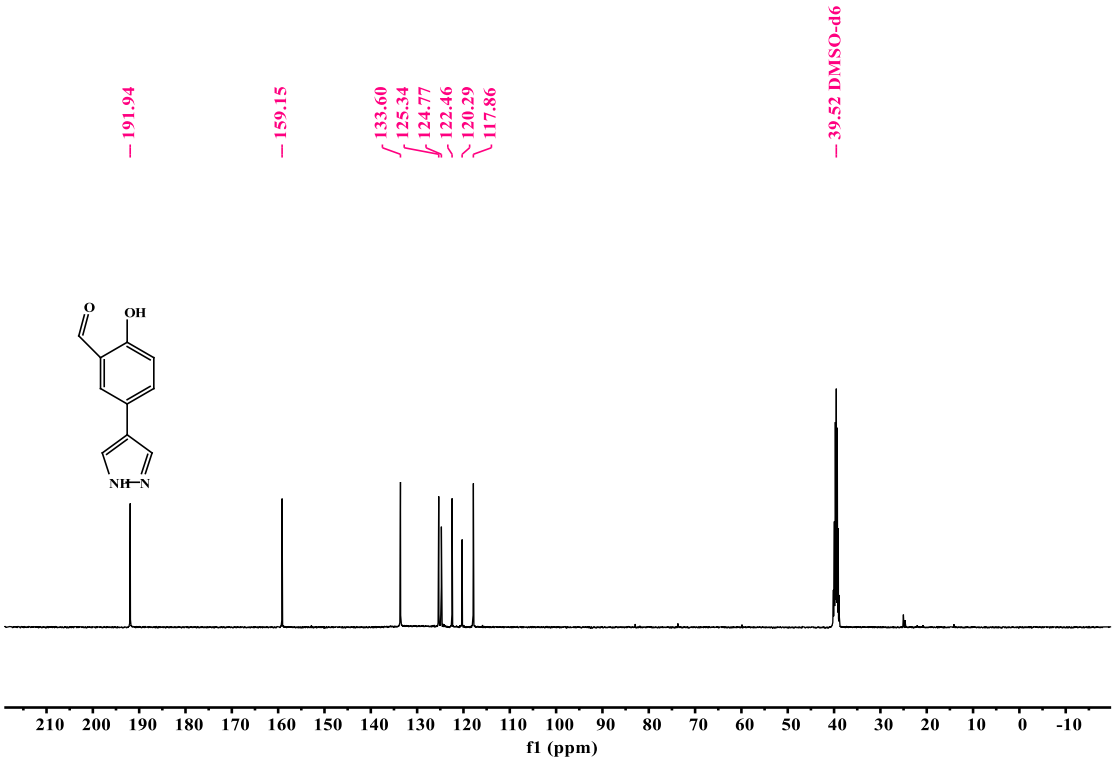

^{13}C spectra of 2-Hydroxy-5-(1H-pyrazol-4-yl)benzaldehyde (6).

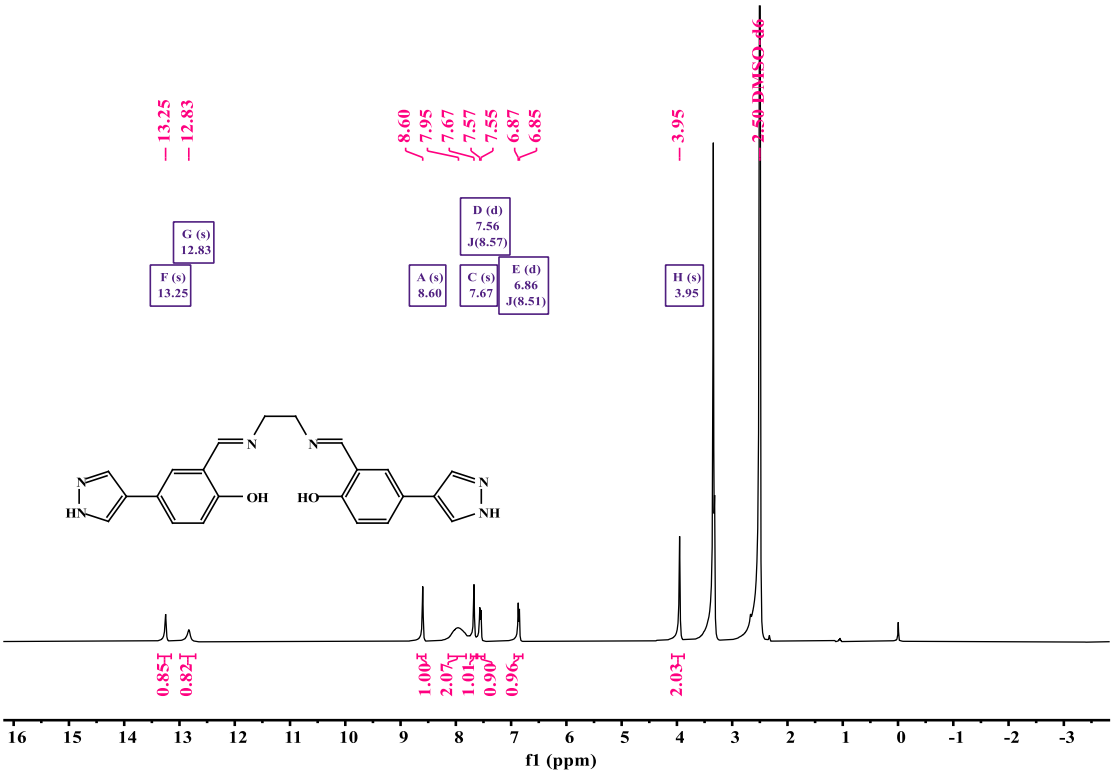

^{1}H spectra of 2,2'-((1E,1'E)-(ethane-1,2-diylbis(azaneylylidene))bis(methaneylylidene))bis(4-(1H-pyrazol-4-yl)phenol) (L_2).

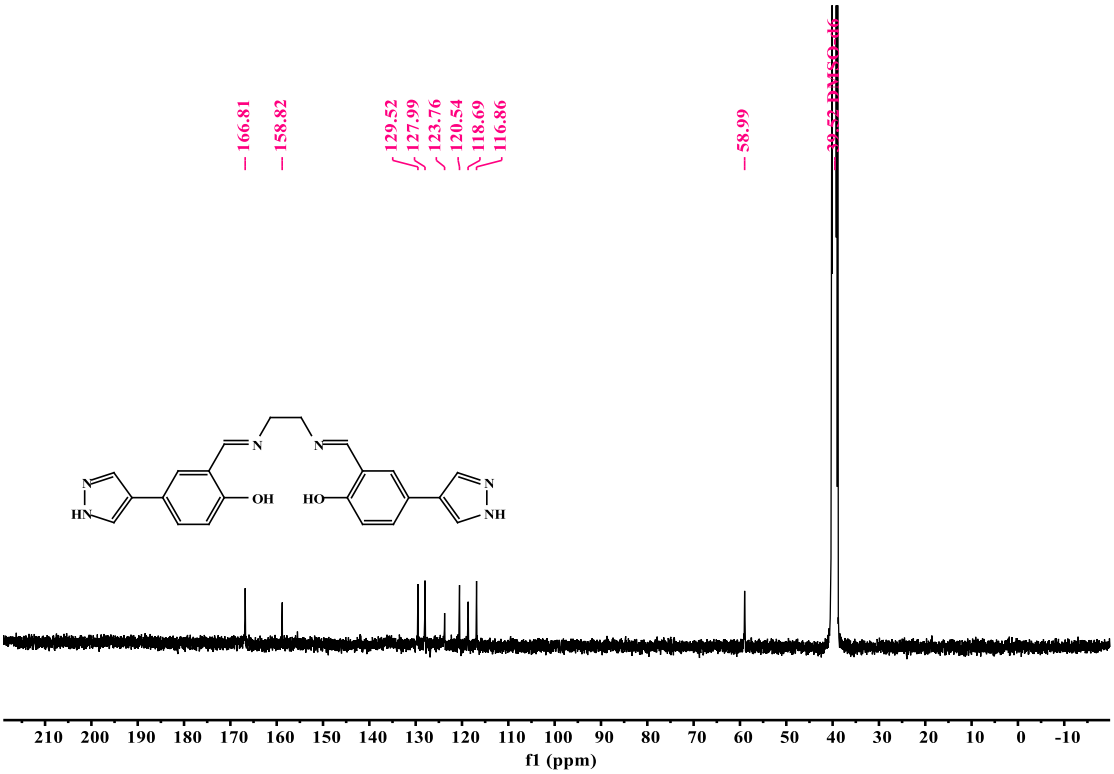

^{13}C spectra of 2,2'-((1E,1'E)-(ethane-1,2-diylbis(azaneylylidene))bis(methaneylylidene))bis(4-(1H-pyrazol-4-yl)phenol) (L_2).

References

1. Z.-J. Li, Y. Ju, Z. Zhang, H. Lu, Y. Li, N. Zhang, X.-L. Du, X. Guo, Z.-H. Zhang, Y. Qian, M.-Y. He, J.-Q. Wang and J. Lin, *Chem. Eur. J.*, 2021, **27**, 17586-17594.
2. J. Zhao, R. Lin, W. Tian, X. Zhu, X. Luo and Y. Liu, *Cryst. Growth Des.*, 2023, **23**, 4417-4423.
3. L. Huang, M. He, B. Chen, Q. Cheng and B. Hu, *ACS Sustain. Chem. Eng.*, 2017, **5**, 4050-4055.
4. J. Li, H. Li, Z. Yuan, J. Fang, L. Chang, H. Zhang and C. Li, *Int. J. Biol. Macromol.*, 2019, **135**, 1171-1181.
5. G. Wang, S. Wang, Z. Sun, S. Zheng and Y. Xi, *Appl. Clay Sci.*, 2017, **148**, 1-10.
6. B. Li, J.-Q. Lv, J.-Z. Guo, S.-Y. Fu, M. Guo and P. Yang, *Bioresour. Technol.*, 2019, **275**, 360-367.
7. A. A. Spagnoli, D. A. Giannakoudakis and S. Bashkova, *J. Mol. Liq.*, 2017, **229**, 465-471.
8. H. Sayğılı and F. Güzel, *J. Clean. Prod.*, 2016, **113**, 995-1004.
9. A. H. Jawad, R. Razuan, J. N. Appaturi and L. D. Wilson, *Surf. Interfaces*, 2019, **16**, 76-84.
10. N. H. Othman, N. H. Alias, M. Z. Shahruddin, N. F. Abu Bakar, N. R. Nik Him and W. J. Lau, *J. Environ. Chem. Eng.*, 2018, **6**, 2803-2811.
11. H. Mittal and S. S. Ray, *Int. J. Biol. Macromol.*, 2016, **88**, 66-80.